Bioconjugate Chemistry

ARTICLE

pubs.acs.org/bc

Synthesis, Characterization, and *In Vitro* Transfection Activity of Charge-Reversal Amphiphiles for DNA Delivery

Xiao-Xiang Zhang,[¶,‡] Carla A. H. Prata,[¶,‡] Jason A. Berlin, Thomas J. McIntosh,[§] Philippe Barthelemy,[†] and Mark W. Grinstaff*

Departments of Biomedical Engineering and Chemistry, Boston University, Boston, Massachusetts 02215, United States

[†]Inserm, U869, Bordeaux, F-33076 France

[‡]Université de Bordeaux, F-33076, Bordeaux, France

[§]Department of Cell Biology, Duke University Medical Center, Durham, North Carolina 27710, United States

Supporting Information

ABSTRACT: A series of charge-reversal lipids were synthesized that possess varying chain lengths and end functionalities. These lipids were designed to bind and then release DNA based on a change in electrostatic interaction with DNA. Specifically, a cleavable ester linkage is located at the ends of the hydrocarbon chains. The DNA release from the amphiphile was tuned by altering the length and position of the ester linkage in the hydrophobic chains of the lipids through the preparation of five new amphiphiles. The amphiphiles and corresponding lipoplexes were characterized by DSC, TEM, and X-ray, as well as evaluated for DNA binding and DNA transfection. For one specific charge-reversal lipid, stable lipoplexes of approximately 550 nm were formed, and with this amphiphile, effective *in vitro* DNA transfection activities was observed.

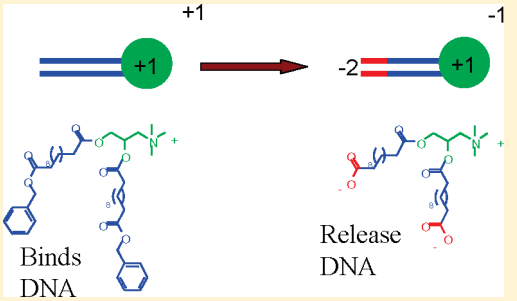

INTRODUCTION

Gene therapy offers the potential to treat a variety of diseases by delivering a functional copy of a missing or defective gene. Current research in this field focuses on two major classes of DNA carriers: viral[1−5] and nonviral.[6−16] Viral vectors transfect a significantly greater percentage of genetic material than nonviral systems, but suffer from a number of drawbacks, including toxicity and induced immunological response.[17] As a consequence, interest in synthesizing and evaluating nonviral delivery systems, including amphiphilic small molecule and polymeric compounds, has increased over the last 10 years. Cationic lipids are one type of amphiphile that can intracellularly transport DNA. Several liposome formulations are commercially available with a few in clinical trials.[16,18] Three examples of such lipids (DOTAP, DOTMA, and DMRIE) are shown in Figure 1.

Following the initial success of these lipids for DNA transfection, a number of different lipid forming complexes of varying structure and composition have been investigated. Within this context, a few representative examples are described below for DNA delivery. The acyl chain length and linker bonds connecting the cationic head to the acyl tail(s) have been varied to enhance transfection efficiency and decrease cytotoxic effects (e.g., DOTMA).[19] Lipospermines, with polycationic headgroups, have been investigated to increase the affinity for DNA.[20] Fluorinated analogues of cationic lipids such as DOTMA have been explored, and these amphiphilies exhibited higher transfection activities *in vitro*[21] and *in vivo*.[22] A hydrophilic spacer (such as PEG) has been placed between the cationic headgroup and the hydrophobic chains[23] to improve transfection efficiency. Researchers have explored the use of glycosidic cationic head groups in an attempt to lower toxicity through tighter interactions with DNA[24−26] or peptide head groups to mimic peptide−DNA binding interactions.[27−30] Recent reports from our laboratory have also described the use of cationic lipids possessing nucleic acid recognition components for nucleic acid delivery in an effort to use more than one type of molecular interaction for complexation.[31−39]

In addition to using these strategies to overcome the low transfection efficiencies of synthetic vectors (estimated to be 0.1% to 1%), functional or stimuli-responsive vectors have also been developed and evaluated. These cationic amphiphiles are able to respond to a stimulus that changes their chemical or physical properties, facilitating DNA delivery. Synthetic vectors have been prepared that are responsive to pH,[40−49] reducing conditions,[50−59] enzymes,[43,60−62] or temperature.[63,64] Many of these functional vectors that degrade or change conformation were designed based on the specific steps in the transfection pathway. This pathway starts with cellular entry of the DNA−amphiphile complex by endocytosis, followed by endosomal escape, and finally nuclear targeting and DNA expression.

Received: October 16, 2010
Revised: March 2, 2011
Published: April 01, 2011

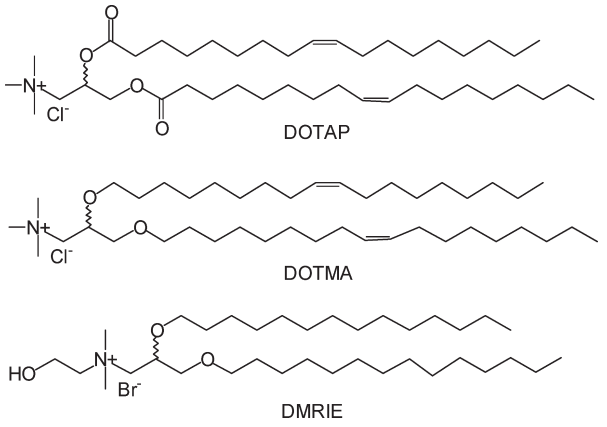

Figure 1. Chemical structures of several common cationic lipids.

Our research effort is centered on the release of DNA from the DNA−amphiphile supramolecular complex following cellular uptake, and as such, we have also focused on functional synthetic vectors. Given that a strong electrostatic assembly is formed between the cationic amphiphile and anionic DNA, and that this assembly is unlikely to disassemble spontaneously, we are interested in altering the electrostatic interaction to free the DNA.[54,65,66] To this end, we have synthesized and characterized new cationic amphiphiles that are capable of undergoing an intracellular electrostatic transition from cationic to anionic under the influence of esterases such as those found in cell lysosomes/endosomes.[67,68] This enables these amphiphiles to release DNA from the supramolecular assembly (Figure 2).

These charge-reversal or charge-switchable amphiphiles possess a positively charged ammonium headgroup that functions to complex DNA and lipophilic acyl chains to promote bilayer formation, similar to other cationic lipids like DOTAP (Figure 1). However, these new amphiphiles also contain ester functionalities near the terminal end of each acyl chain that, upon hydrolysis, switch the overall charge of the amphiphile from positive to negative. As an extension of our previous communication[54] in which we introduced the charge-reversal amphiphile, in this manuscript we have synthesized and investigated nine amphiphiles possessing C10, C12, or C16 acyl chain lengths terminally protected by benzyl, ethyl, butyl, or acetyl groups (Figure 3). The optimal chain length and terminal groups were determined based on amphiphile−DNA binding and DNA release. Standard ethidium bromide assays established the DNA binding capability of each of the vectors over a range of pH. The release of DNA from the DNA−amphiphile assembly was monitored also using an ethidium bromide assay. To determine the thermal and structural properties of the lipid and DNA−lipid complexes, differential scanning calorimetery (DSC), dynamic light scattering (DLS), transmission electronic microscopy (TEM), and X-ray diffraction were performed. Finally, the transfection of the amphiphile/DNA complexes was evaluated *in vitro* in several cell lines.

EXPERIMENTAL PROCEDURES

Please see the Supporting Information for complete experimental details.

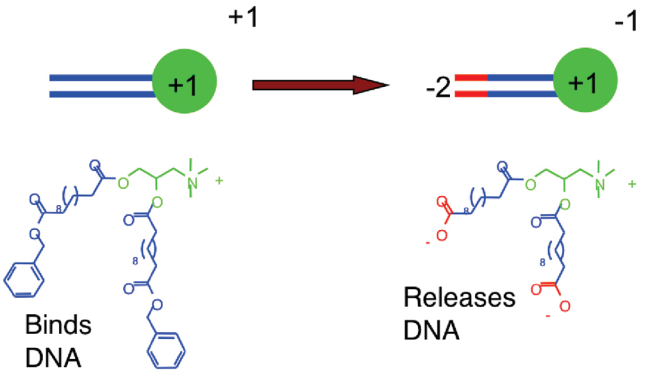

Figure 2. Charge-reversal or charge- switchable effect of the amphiphiles.

RESULTS AND DISCUSSION

To bind DNA, form lipoplexes, and then eventually release DNA, each amphiphile requires three distinct structural components: a cationic headgroup, hydrophobic chains, and terminal ester linkages. As shown in Figure 3, amphiphile **1** has a cationic headgroup to bind DNA, lipophilic acyl chains to form a bilayer, and ester linkages at the end of the acyl chains for enzymatic hydrolysis. We prepared the series of compounds **2**−**10**, shown in Figure 3, to systematically assess the role of each structural component and to evaluate the effects of amphiphile structure and reactivity (chain length, terminal end group, and ester or amide terminal group) on DNA binding/release, supramolecular assembly, and gene delivery efficacy. Specifically, amphiphile **1** possesses a cationic ammonium headgroup and two dodecanoic acid chains protected with benzyl esters. Hydrolysis of the benzyl esters of **1** affords compound **2**, which is negatively charged at neutral pH. Amphiphile **3** is an analogue of **1** that possesses noncleavable amide linkages, whereas compound **4** lacks the long acyl chains completely. Amphiphiles **6** and **7** are short and long acyl chain analogues of **1**, respectively, with the same terminal benzyl ester group. Amphiphiles **8** and **9** possess terminal alkyl ester linkages of two different chain lengths (ethyl and butyl ester, respectively). Finally, amphiphile **10** contains a similar terminal ester but upon hydrolysis affords two hydroxyl terminated acyl chains and thus remains cationic at neutral pH in aqueous solution.

The synthetic route to the amphiphiles is shown in Scheme 1. The preparation requires the use of functionalized fatty acids. The monoprotected benzyl ester fatty acids were prepared from the corresponding diacids (decanoic, dodecanoic, or hexanoic) with benzyl formate in the presence of Dowex 50W-X2 in octane at 80 °C. The butyl ester fatty acid was prepared in a similar manner using butyl formate. The ethyl ester fatty acids were obtained by the addition of ethanol to a solution of dodecanedioyl dichloride in tetrahydrofuran in the presence of triethylamine at 0 °C. The benzyl amide analogue was prepared in a similar manner using benzylamine. The acetylated fatty acid was prepared by acetylation of the hydroxydodecanoic acid using acetic anhydride in pyridine. Next, the monofunctionalized fatty acid derivatives were coupled to 3-dimethylaminopropanediol in the presence of DCC and DMAP in dichloromethane. The reaction yields ranged from 80% to 95% for all steps. Finally, the amphiphiles were reacted with methyl iodide in dichloromethane to quaternize the tertiary amine in quantitative yield. Complete details of the synthesis for each compound are found in the Supporting Information.

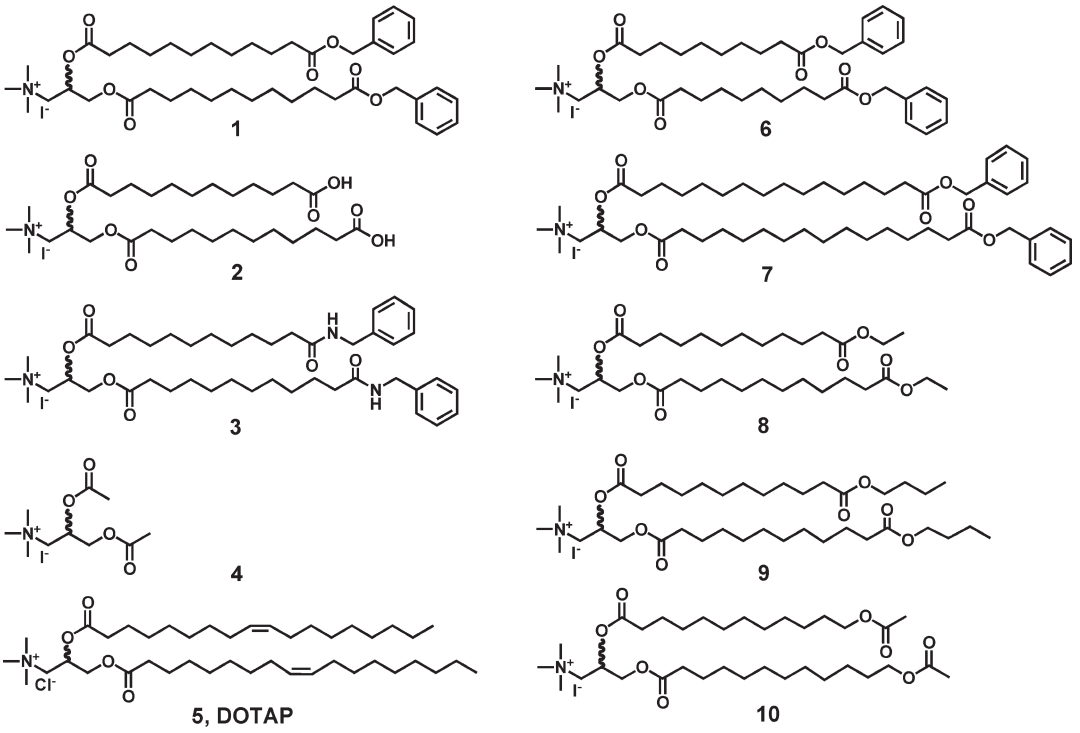

Figure 3. Structures of the charge-reversal amphiphiles under investigation for gene delivery.

Scheme 1. Synthesis of the Charge-Reversal Amphiphiles

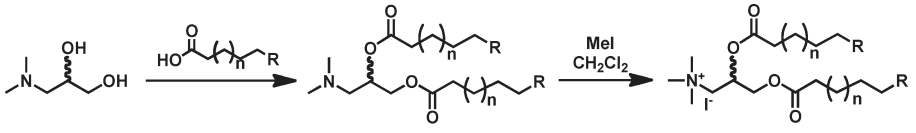

1: n = 7; R = C(O)OBn
2: n = 7; R = C(O)OH
3: n = 7; R = C(O)NHBn
4: acetate derivative
6: n = 5; R = C(O)OBn
7: n = 11; R = C(O)OBn
8: n = 7; R = C(O)OEt
9: n = 7; R = C(O)OBu
10: n = 7; R = OC(O)CH3

As the first step toward evaluating these amphiphiles for the delivery of nucleic acids, we used an ethidium bromide displacement assay to determine whether the amphiphiles bind DNA.[69] This fluorescence quenching assay is an indirect method to measure DNA binding by monitoring the displacement of the ethidium bromide from DNA by the cationic amphiphile. This assay is widely used to assess small molecule/DNA binding, and it is assumed that the small molecule binder is responsible for displacing ethidium bromide and causing fluorescence decrease.

As shown in Figure 4, the fluorescence intensity decreases for amphiphiles **1**, **3**, **6**−**10**, and DOTAP upon addition to the ethidium bromide−DNA solution, but does not decrease for amphiphiles **2** and **4**. Amphiphile **2** possesses an overall negative charge and, consequently, does not bind DNA due to unfavorable electrostatic interactions. Compound **4** is a cationic amphiphile but does not bind DNA, indicating the importance of the hydrophobic acyl chains for the formation of a strong interaction with DNA.

The different terminal ester groups (ethyl, butyl, benzyl, acetyl) of the cationic amphiphiles do not appear to have a significant effect on DNA binding, as all of the amphiphiles bind DNA. The binding constants can be estimated and compared by measuring the loss of EtBr fluorescence as a function of the vector added. The concentration which produces 50% of the inhibition of fluorescence (IC_{50}) approximates the binding constant. The apparent binding constants were calculated as follows: $K_{app} = (1.26 \times 10^{-6}/\ IC_{50}) \times K_{EtBr}$ with $K_{EtBr} = 10^7\ M^{-1}$ as described elsewhere.[70] The binding constant for all the amphiphiles is on the order of $10^6\ M^{-1}$ and similar in magnitude to DOTAP ($K = 10^6\ M^{-1}$). These binding curves indicate that a ~1:1 charge complex is formed between DNA and most of these amphiphiles, except for **7**, which forms a ~ 2:1 charge complex with DNA.

We next determined the effect of pH on DNA binding for amphiphiles **1** and **2**. We chose two pH conditions near physiological pH (pH 7 and 8) and a lower pH of 5.5 that mimics the conditions of the early endosome. Figure 5 shows the fluorescence intensity as a function of amphiphile/DNA charge ratio for amphiphiles **1**, **2**, and **5** (DOTAP) at the three different pH conditions. The fluorescence intensity decreases as a function of charge ratio for both amphiphile **1** and DOTAP across all three

pHs. The binding curves look similar, with a 1:1 charge complex being formed between the amphiphile and DNA. The fluorescence intensity is constant and does not decrease for amphiphile **2**, indicating that **2** does not displace EtBr from DNA. This result is consistent with **2** being anionic over this pH range and as that the pK_a for the terminal carboxylic acids is below 5.5. Overall, these pH conditions do not play a significant role in DNA binding of the amphiphiles.

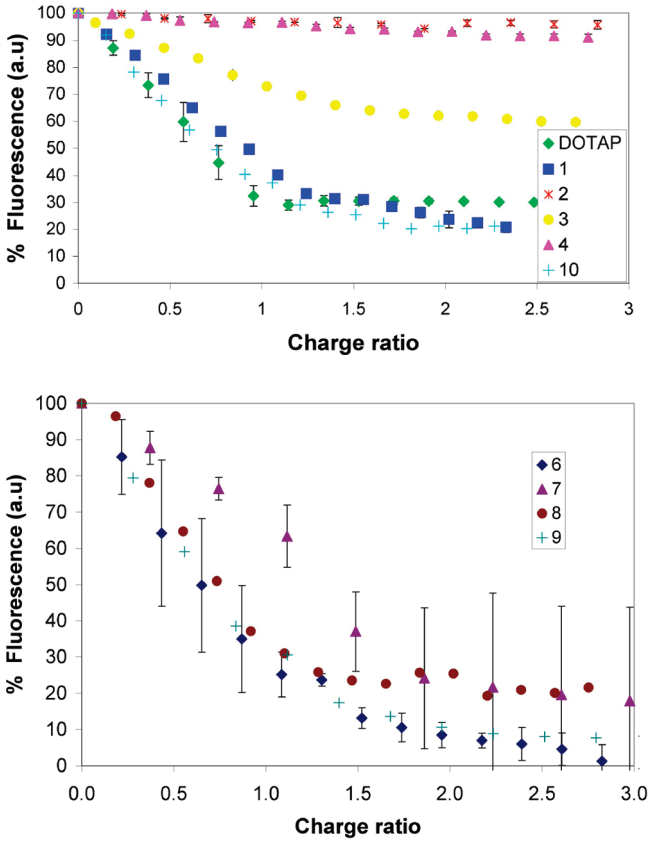

Figure 4. (top) Fluorescence intensity as a function of amphiphile/DNA charge ratio. (bottom) The fluorescence intensity as a function of amphiphile/DNA charge ratio for amphiphiles **1**, **6**−**10**, and DOTAP. N = 3 Avg ± SD.

To evaluate the release of the DNA from the amphiphile−DNA complex, the amphiphile/EtBr/DNA solution was incubated with a porcine liver esterase at pH 7.4 (1000 units/mL; 37 °C; 100 mM NaCl, 100 mM Tris buffer). For these release studies, the fluorescence intensities as a function of time for the various amphiphiles (including DOTAP) are shown in Figures 6 and 7. The increase in fluorescence from EtBr results from reintercalation of EtBr in the DNA; once the DNA is "free" from the amphiphile complex, ethidium bromide can bind with the DNA. As shown in Figure 6, amphiphile **1** no longer binds strongly to the DNA as a consequence of hydrolysis of its terminal benzyl esters. This result is consistent with the binding studies conducted with **2**, the hydrolyzed product of **1** prepared independently. However, in the presence of the enzyme, no increase in fluorescence over time is observed with amphiphile **3** or **5** (DOTAP), which possesses a terminal amide linkage or methyl group, respectively. A slightly slower increase in fluorescence is observed with compound **10**, which upon hydrolysis affords a neutral hydroxyl group.

To confirm that enzymatic hydrolysis cleaved the benzyl ester bond, liposomes formed from amphiphile **1** were incubated in PBS at 37 °C in the presence of porcine liver esterase, and the reaction products were examined by LC-MS. The results show that, within 30 min, ∼58% of **1** had converted to the hydrolyzed product **2**, and **1** was completely hydrolyzed by 2.5 h.

When the terminal ester is changed from a benzyl to an ethyl group as in compound **8**, similar EtBr−DNA binding curves to those of compound **1** are obtained (Figure 7). The increases in fluorescence indicate that both benzyl and ethyl terminal esters are readily hydrolyzed. Likewise, similar results are obtained when the acyl chain length is shortened from C12 to C10 (**1** vs **6**) while maintaining the terminal benzyl esters. However, upon extending the acyl chain length to C16 from C12 (**1** vs **7**), no increase in fluorescence is observed. Our interpretation of this

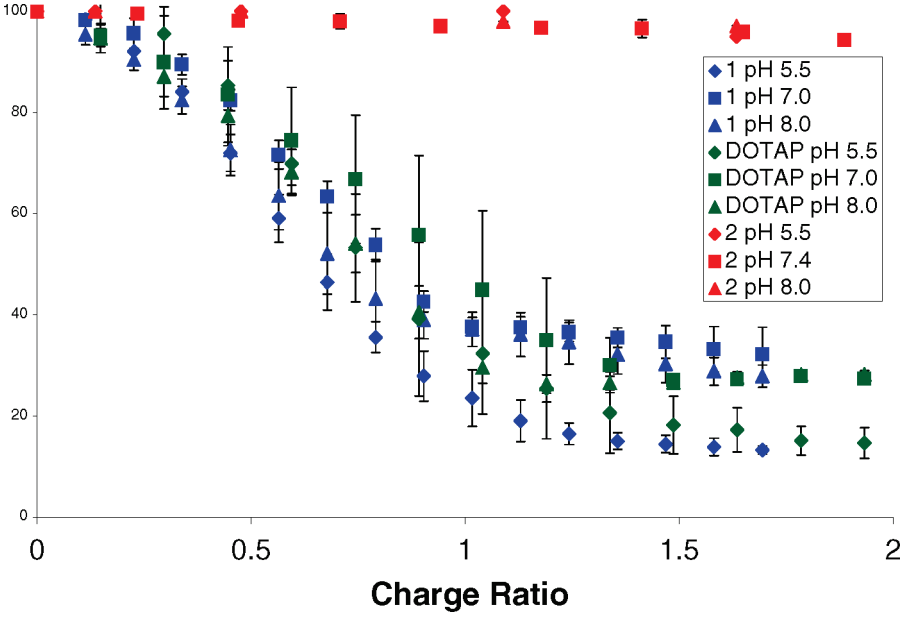

Figure 5. Fluorescence intensity as a function of amphiphile/DNA charge ratio in pH solutions of 5.5, 7.0 and 8.0. N = 3 Avg ± SD.

dx.doi.org/10.1021/bc1004526 |*Bioconjugate Chem.* 2011, 22, 690–699

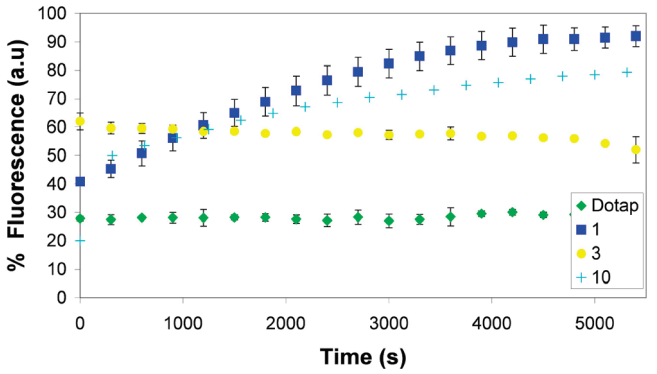

Figure 6. Ethidium bromide intercalation assay showing the fluorescence intensity as a function of time in the presence of a porcine liver esterase (1000 units/mL). $N = 3$ Avg ± SD.

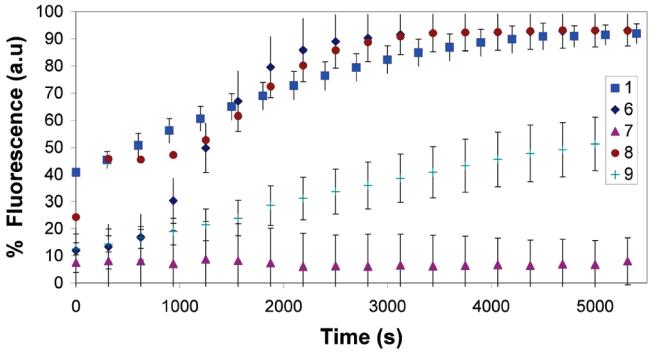

Figure 7. Ethidium bromide intercalation assay showing the fluorescence intensity as a function of time in the presence of a porcine liver esterase. $N = 3$ Avg ± SD.

result is that the long chain analogue forms a more stable bilayer structure, reducing accessibility of the ester bonds to the enzyme, and therefore inhibiting hydrolysis. The phase-transition temperature (T_m) for **7** is 23 °C higher than for **1**, as shown in Table 1, which is consistent with this interpretation. Upon changing the benzyl to an ethyl ester but maintaining the chain length of C12, we observe a similar rate of hydrolysis (**6** vs **8**). However, **9**, which possesses an *n*-butyl ester as opposed to an ethyl ester (**9** vs **1**), shows a slower rate of fluorescence increase during the assay. In this amphiphile, the hydrolyzable ester is buried further in the hydrophobic chain, leading to a slower rate of hydrolysis. The enzymatic mechanism is still unknown, although we suspect that, during the flip-flop of the lipids, the enzyme hydrolyzes the terminal ester bonds.

Overall, the fluorescence data indicate that release of DNA from the supramolecular assembly does not occur for amphiphiles lacking a terminal hydrolyzable ester linkage, and those linkages near the headgroup or buried deeper in the chain are less accessible to enzymatic hydrolysis. The data also show the difference in DNA release from an amphiphilic complex that generates a resulting anionic amphilphile product versus a neutral one (**1** vs **10**).

Next, transfection experiments using the reporter gene, β-galactosidase (β-gal, pVax-LacZ1, Invitrogen), were performed with Chinese hamster ovarian (CHO) cells. The reporter gene was first mixed with the cationic lipid, at a defined amphiphile/DNA ratio, in potassium phosphate buffer (PBS) at room temperature.

Table 1. DSC Results for the Amphiphile Assemblies

compound	T_m (°C)	ΔH (kcal/mol)
1	52.55	2.03
6	46.32	3.18
7	75.45	1.57
8	78.44	8.47
9	76.14	3.78
10	50.77	0.102

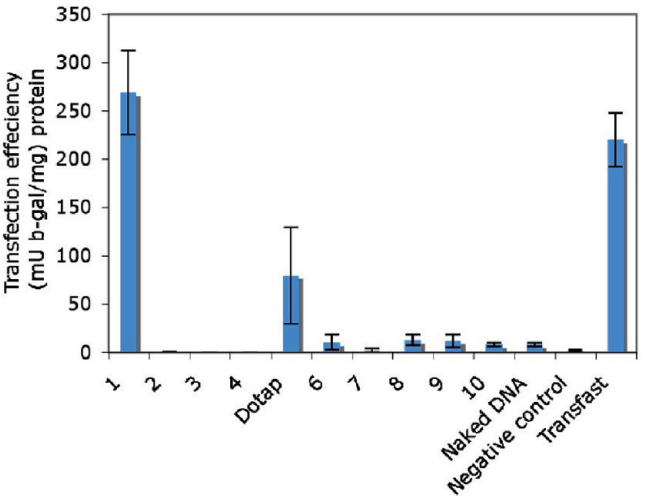

Figure 8. Transfection efficiency of the different amphiphiles in CHO cells. $N = 3$ Avg ± SD.

The complexes were added to CHO cells after 15 min. The amount of DNA used was the same as was used in the naked DNA control (no amphiphile) and positive control experiments (DOTAP and Transfast). The negative control was amphiphile **1** without DNA. After incubation at 37 °C and 5% CO_2 for 2 h, the solution containing the lipoplexes was removed and fresh growth medium with serum was added. Transfection efficiencies were assessed after 48 h using the β-galactosidase enzyme assay in conjunction with a standard curve. The efficacy of each transfection was calculated as β-gal activity normalized to total protein. We first performed a screen to identify the optimal amphiphile **1**/DNA ratio for greatest transfection examining ratios of 1:1, 2:1, 5:1, 10:1, 15:1, and 45:1. We also varied the time of incubation of the lipoplex with the cells from 30 min to 3 h, as well as performed analyses at the 24 and 48 h time points. On the basis of these experiments, the highest transfection efficiency was at a 5:1 ratio, an exposure time of 2 h, and analysis after 48 h. With these optimal conditions, we then performed a series of transfection experiments with the charge-reversal amphiphiles, as summarized in Figure 8. Amphiphile **1** was the most effective vector for transfection. The other compounds (**2**−**4** and **6**−**10**) showed minimal transfection activity, comparable to the negative control and naked DNA. The transfection efficacy of amphiphile **1** was significantly better than that of DOTAP ($p < 0.05$) and comparable to that of Transfast ($p > 0.05$). In the literature, it has also been shown that the addition of neutral lipids (i.e., helper lipids) such as dioleylphosphatidylethanolamine (DOPE) to a cationic lipid formulation can

dx.doi.org/10.1021/bc1004526 |*Bioconjugate Chem.* 2011, 22, 690–699

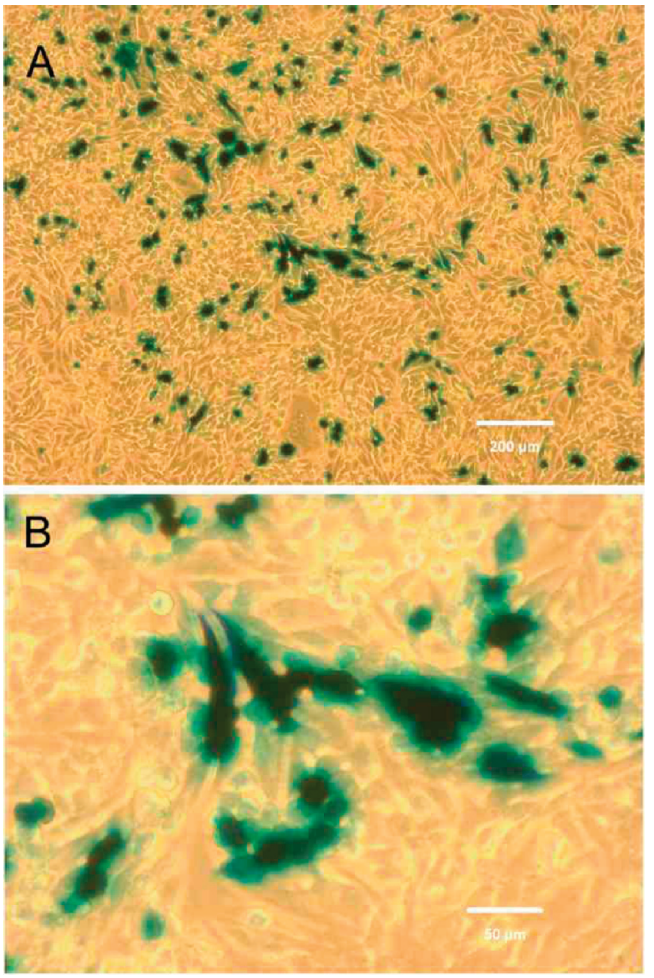

Figure 9. Photograph of β-galactosidase transfected cells using amphiphile **1** at low and high magnification. Dark blue stain represents B-gal expression.

improve DNA transfection efficiency.[19] Consequently, the above transfection experiments were repeated using the helper lipid, DOPE, and the charge-reversal amphiphiles at a 1:1 ratio. No increase in transfection efficiency was observed for these conditions (data not shown).

Micrographs of the β-galactosidase transfected CHO cells using amphiphile **1** are shown in Figure 9. This transfection experiment was conducted in a similar manner except it was done on a glass slide that had been previously modified with collagen to anchor the cells. The cells are expressing the protein β-gal (dark blue stain), and there appear to be few patches containing no cells, indicating minimal toxicity under these experimental conditions. This lack of cytotoxicity was quantitatively determined in our next set of experiments.

Cytotoxicity experiments were performed with CHO cells using both a formazan-based proliferation assay and a total protein assay. The cells were seeded onto a 96-multiwell microliter plate with an approximate density of 1×10^4 cells per well. The compounds were added to the cells 24 h later. After 24 h, cell proliferation was determined and expressed as a percentage of nontreated cells as shown in Figure 10. None of the amphiphiles showed a significant cytotoxicity, with values similar to the negative control (i.e., nontreated cells).

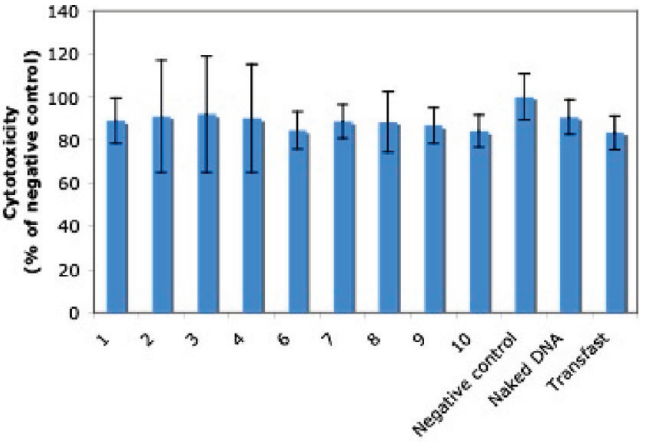

Figure 10. Cytotoxicity of the different lipids in CHO cells. $N = 3$ zAvg $\pm$ SD.

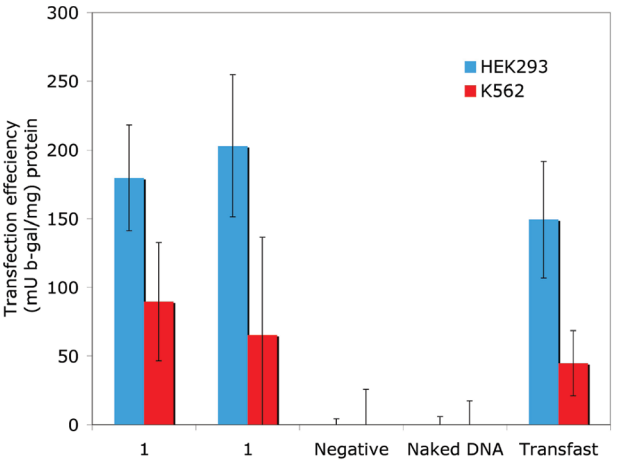

Figure 11. Transfection efficiency of amphiphile **1** with HEK293 and K562 cell lines. $N = 3$ Avg $\pm$ SD. First data set with **1** is at 15:1 and the second data set is at 45:1 charge ratio.

With these encouraging results, we then evaluated the transfection activity of amphiphile **1** in four other cell lines. Transfection experiments using human embryonic kidney (HEK293), erythroleukemic (K562), mouse fibroblast (NIH 3T3), and human liver carcinoma (HepG2) cell lines were performed with compound **1** (see Figure 11). Once again, we varied amphiphile **1**/DNA ratio, and only at high amphiphile/DNA ratio did we observe transfection (HEK 15:1; K562 45:1). Amphiphile **1** transfected DNA with similar efficiency to Transfast in the HEK293 and K562, but we did not observe significant transfection in the NIH 3T3 or HepG2 lines (data not shown).

With the above transfection activities recorded, we embarked on a series of physiochemical experiments to elucidate the key structural and physical properties of amphiphile **1** likely responsible for transfection activity. Given the polar headgroup and long hydrophobic acyl chains present in amphiphile **1**, it is likely to form bilayer structures in aqueous solution. To test this idea, differential scanning calorimeter (DSC), dynamic light scattering (DLS), transmission electron microscopy (TEM), and X-ray diffraction (XRD) experiments were performed. The samples were prepared for these studies by introducing a chloroformic

solution of amphiphiles into a pear-shaped flask. The solution was evaporated under vacuum, leaving a thin film deposited onto the flask wall. A total of 1 mL Tris buffer (100 mM Tris, 100 mM NaCl, pH 7.4) was then added, and the film was peeled off by vortexing. After 20 extrusions though a 50 nm polycarbonate membrane (Avanti Polar Lipids), the milky aqueous suspension turned into a homogeneous solution. The lipoplexes were prepared in an analogous manner by addition of the DNA to the previously prepared liposome solution.

DSC traces of the aqueous hydrated amphiphiles (**1**, **6**−**10**) show for each lipid a single phase-transition temperature (T_m). The T_m and transition enthalpy (ΔH) vary as the chain lengthens (C10, C12, and C16; **6** vs **1** vs **7**, respectively) when the end groups remain the same. For example, the T_m increases from 46 °C for **6** to 75 °C for **7**, indicating that amphiphile **7** forms a more stable structure than **1** or **6**. This trend with increasing chain length and higher T_m is true for T_m, but not for enthalpy. The enthalpy is smaller for **7** than for **6** or **1**. These results are consistent with reports on other lipid families (e.g., phosphatidylcholine and Avanti polar technical data). When the chain lengths are kept constant but the end group is changed from a benzyl to an alkyl ester on the amphiphile (e.g., **1** vs **8**), the T_m and enthalpy increase by about 25 °C. On the other hand, reversing the directionality of the ester linkage (**10** vs **8**) leads to a decrease in the T_m, possibly reflecting the greater ease that water molecules can hydrate and destabilize the terminal chain end group in **8** relative to **10**. In all, the DSC data showed that these charge-reversal lipids form organized structures with melting temperatures higher than 0 °C, the melting temperature of DOTAP, a common amphiphile used for gene transfection.

The mean diameter of the supramolecular structures formed by the different amphiphiles and by the amphiphile/DNA complexes was measured by dynamic light scattering (DLS). Compound **1** formed structures with a mean diameter of 110 nm, and the diameter increased to 562 nm in the presence of DNA. Amphiphile **6** formed structures with the same mean diameter (110 nm) and in presence of DNA formed structures with a mean diameter of 680 nm. Compounds **8** and **9** formed aggregates of 1 μm and larger in diameter as measured by DLS. Likewise, compounds **2**, **3**, **7**, and **10** afforded very large aggregates and precipitated products.

At 22 °C, X-ray diffraction patterns of amphiphile **1** in the absence of DNA gave three orders of a lamellar repeat period of 5.22 ± 0.03 nm with a sharp wide-angle spacing of 0.46 ± 0.01 nm. These data indicate that compound **1** formed gel-phase multibilayers at 22 °C, consistent with the DSC data (Table 1). In the presence of DNA, fully hydrated amphiphile **1** gave a lamellar repeat period of 5.31 ± 0.14 nm with a sharp wide-angle spacing of 0.46 ± 0.01 nm. Thus, the presence of the DNA did not significantly change d, indicating that the DNA was not intercalated between the lipid layers. Typically, an increase of 1 to 1.4 nm in d is observed with formation of a DNA−lipid sandwich structure.[71] These XRD data suggest a model where the DNA is entrapped at the surface or at the interface between the multilamellar vesicles (MLVs) in solution. This model is consistent with the increase in size observed by DLS, which could be caused by DNA bridging between these large MLVs. We were able to obtain a TEM image of amphiphile **1** in the presence, but not the absence, of DNA. The TEM micrograph showed multilamellar structures with an average vesicle diameter of 200 nm (Figure 12). Repeated attempts to obtain X-ray data on **6** in the presence and absence of DNA were unsuccessful.

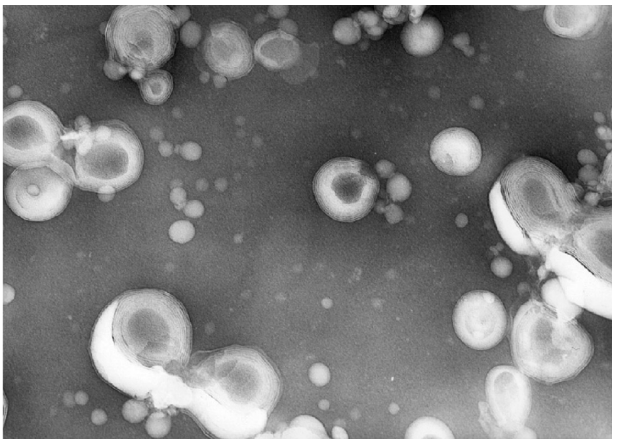

Figure 12. TEM micrographs of amphiphile **1** in aqueous solution, negative staining with ammonium molybdate 1% in water.

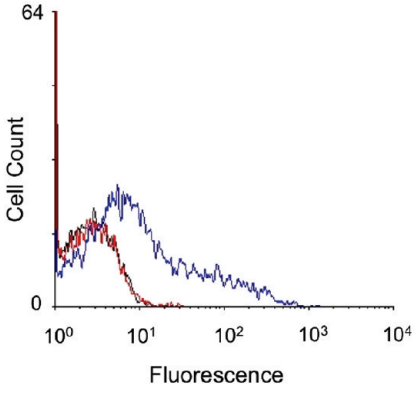

Figure 13. Flow cytometry histogram for CHO cells transfected with rhodamine-labeled DNA using either **1** (blue) or **6** (red). Negative control (black).

Of the amphiphiles, compound **6** has a melting temperature slightly lower than **1** and forms similarly sized structure by DLS as **1**, but does not give high transfection activity. We subsequently examined if the difference in activity between **1** and **6** was related to the amount of lipoplex taken up by the CHO cells. Cells were transfected with rhodamine-labeled DNA using either **1** or **6**, and the resulting cellular rhodamine fluorescence signal was recorded by flow cytometry. As shown in Figure 13, a significant amount of fluorescence was observed when DNA was delivered using **1**, while the fluorescence signal was almost the same as that of the negative control when delivered using **6**. Cell population analysis revealed that 27% of the cells were rhodamine-positive when transfected with **1**, compared to only 0.5% cells when transfected with **6**. These data suggest that the difference in cellular uptake may be responsible for the difference in the transfection activity between **1** and **6**. The underlying mechanism for the difference in cellular uptake is unknown and currently under investigation, but **6** does form a relatively weaker supramolecular structure than **1** as evident by the lower T_m.

Altogether, the results suggest a number of key findings responsible for the higher transfecton activity observed with amphiphile **1** compared to compounds **2**−**10**. First, compounds **2** and **4** do not bind DNA, while amphiphiles **1**, **3**, and **5**−**10** do bind DNA, at roughly the same magnitude. Amphiphiles **1**, **6**, **8**,

and **10** release DNA relatively rapidly in the presence of an esterase compared to the amphiphile **9**. Amphiphiles **3**, **5** (DOTAP), and **7** do not release DNA in the presence of an esterase. Amphiphiles **3**, **7**, **8**, **9**, and **10** formed aggregates of 1 μm or larger in diameter. Amphiphiles **1** and **6** both form similarly sized nanometer lipoplexes; however, more lipoplexes formed with amphiphile **1** are taken up by CHO than **6**.

In summary, *in vitro* gene delivery using charge reversal or charge switchable amphiphiles is a new approach and, like other functional delivery systems, provides a means to increase transfection activity, as well as potentially new reagents to study the transfection pathway. These amphiphiles were designed to transform from a cationic species that binds DNA to an anionic species that loses affinity to DNA after cleavage by an esterase. This charge-reversal effect would release DNA from the supramolecular complex. To evaluate the role of key amphiphile structural components, we synthesized in good yield a series of amphiphiles to determine the physicochemical properties and transfection efficiency of these amphiphiles. This series of amphiphiles included those that had C10 to C16 chains and a benzyl, *n*-butyl, or ethyl ester terminal group, as well as amphiphiles possessing very short alkyl chains and chains terminated with a carboxylate. All of these amphiphiles bind DNA and form amphiphile/DNA assemblies except for the compounds lacking long hydrophobic chains or those terminated with a carboxylate. The DNA release from the complexes and the dissociation rate of the complexes is controlled by the chemical structure of the lipid, which plays an important role in the stability and organization of the resulting supramolecular assembly. For example, the enzymatic hydrolysis rate of the ester linkage was dependent on hydrophobicity of the amphiphile, as the rate of hydrolysis was faster for the ethyl than the *n*-butyl analogue. The XRD data showed that amphiphile **1** forms bilayer organizations in the presence and absence of DNA, and DLS and TEM data showed that this amphiphile formed vesicles and lipoplexes with DNA on the order of 550 nm. The other amphiphiles organized themselves in larger aggregates. DSC data showed that the melting temperatures were between 45 and 80 °C, with those amphiphiles possessing the longer alkyl chains having higher melting temperatures.

The transfection experiments showed that the highest DNA transfection activity was observed for amphiphile **1**. This activity was observed in three different cell lines—Chinese hamster ovarian (CHO), human embryonic kidney (HEK293), and erythroleukemic (K562) cells. All other amphiphiles (except DOTAP and Transfast) showed minimal transfection activity, comparable to that of the negative control. Further studies will investigate the mechanism of cellular uptake and DNA delivery to the nucleus. This concept of charge reversal or charge switching has been successfully extended to additional cationic lipid structures,[66] zwitteronic lipids,[65] ferrocene-containing lipids,[55,56] and polymers[41,72] for DNA transfection, suggesting that this is an important, and potentially general, approach. Our data show that charge-reversal amphiphile **1** has all of the characteristics necessary for DNA delivery: it binds DNA, releases DNA upon charge reversal, forms well-ordered bilayers, forms lipoplexes of nanometer size, is taken up by cells, and efficiently transfects several cell types.

■ ASSOCIATED CONTENT

Ⓢ Supporting Information. Experimental procedures, fluorescence studies, DNA transfection, and cytotoxicity data. This material is available free of charge via the Internet at http://pubs.acs.org.

■ AUTHOR INFORMATION

Corresponding Author

*Corresponding author. E-mail: mgrin@bu.edu.

Author Contributions

¶Contributed equally to the work.

■ ACKNOWLEDGMENT

This work was supported by the Army Research Office (PB) and Grants GM27278 (TJM) and EB005658 (MWG) from the National Institutes of Health. We thank Dr. Dan Luo and Erin King for helpful discussions and technical advice at Cornell University. We thank Mr. Yuxing for help with the initial studies. We also thank Drs. Jun-lin Guan and Zara Melkoumian for providing the cell lines, and Dr. Stephen Lee (ARO) for support and discussions.

■ REFERENCES

(1) Deregowski, P., and Canalis, E. (2008) Gene delivery by retroviruses. *Methods Mol. Biol. 455*, 157–162.

(2) Flotte, T. R. (2004) Gene therapy progress and prospects: Recombinant adeno-associated virus (rAAV) vectors. *Gene Ther. 11*, 805–810.

(3) Lundstrom, K. (2004) Gene therapy applications of viral vectors. *Technol. Cancer Res. Treatment 3*, 467–477.

(4) Flotte, T. R. (2007) Gene therapy: The first two decades and the current state-of-the-art. *J. Cell. Physiol. 213*, 301–305.

(5) Ozawa, K. (2007) Gene therapy using AAV vectors. *Drug Delivery Syst. 22*, 643–650.

(6) Mintzer, M. A., and Simanek, E. E. (2009) Nonviral vectors for gene delivery. *Chem. Rev. 109*, 259–302.

(7) Ewert, K. K., Ahmad, A., Bouxsein, N. F., Evans, H. M., and Safinya, C. R. (2008) Non-viral gene delivery with cationic liposome-DNA complexes. *Methods Mol. Biol. 433*, 159–175.

(8) Wolff, J. A., and Rozema, D. B. (2007) Breaking the bonds: non-viral vectors become chemically dynamic. *Mol. Ther. 16*, 8–15.

(9) Wong, S. Y., Pelet, J. M., and Putnam, D. (2007) Polymer systems for gene delivery-past, present, and future. *Prog. Polym. Sci. 32*, 799–837.

(10) Dang, J. M., and Leong, K. W. (2006) Natural polymers for gene delivery and tissue engineering. *Adv. Drug Delivery Rev. 58*, 487–499.

(11) Christine, C. C., and Huang, L. (2005) Recent advances in non-viral gene delivery. *Adv. Genetics 53*, 3–18.

(12) Reineke, T. M., and Grinstaff, M. W. (2005) Designer materials for nucleic acid delivery. *Mat. Res. Soc. Bull. 30*, 635–639.

(13) Luo, D., and Saltzman, W. M. (2000) Synthetic DNA delivery systems. *Nat. Biotechnol. 18*, 33–37.

(14) Kabanov, A. V., Felgner, P. L., and Seymour, L. W. (1998) *Self-assembling complexes for gene delivery: From laboratory to clinical trial*, John Willey and Sons, New York.

(15) Behr, J. P. (1994) Gene transfer with synthetic cationic amphiphiles: prospects for gene therapy. *Bioconjugate Chem. 5*, 382–389.

(16) Miller, A. D. (1998) Cationic liposomes for gene therapy. *Angew. Chem. Int. 37*, 1768–1785.

(17) Marshall, E. (2000) Clinical research - FDA halts all gene therapy trials at Penn. *Science 287*, 565–567.

(18) Felgner, P. L., Gadek, T. R., Holm, M., Roman, R., Chan, H. W., Wenz, M., Northrop, J. P., Ringgold, G. M., and Danielsen, M. (1987) Lipofectin: A highly efficient, lipid mediated DNA-transfection procedure. *Proc. Natl. Acad. Sci. U.S.A. 84*, 7413–7417.

(19) Felgner, J. H., Kumar, R., Sridhar, C. N., Wheeler, C. J., Tsai, Y. J., Border, R., Ramsey, P., Martin, M., and Felgner, P. L. (1994) Enhanced gene delivery and mechanism studies with a novel series of cationic lipid formulations. *J. Biol. Chem. 269*, 2550–2561.

(20) Behr, J. P., Demeneix, B., Loeffler, J. P., and Perez-Mutul, J. (1989) Efficient gene transfer into mammalian primary endocrine cells with lipopolyamine coated DNA. *Proc. Natl. Acad. Sci. U.S.A. 86*, 6982–6986.

(21) Gaucheron, J., Santaella, C., and Vierling, P. (2002) Transfection with fluorinated lipoplexes based on fluorinated analogues of DOTMA, DMRIE and DPPES. *Biochim. Biophys. Acta — Biomembr. 1564*, 349–358.

(22) Boussif, O., Gaucheron, J., Boulanger, C., Santaella, C., Kolbe, H. V. J., and Vierling, P. (2001) Enhanced in vitro and in vivo cationic lipid-mediated gene delivery with a fluorinated glycerophosphoethanolamine helper lipid. *J.Gene Med. 3*, 109–114.

(23) Schulze, U., Schmidt, H., and Safinya, C. R. (1999) Synthesis of novel cationic poly(ethylene glycol) containing lipids. *Bioconjugate Chem. 10*, 548–552.

(24) Bessodes, M., Dubertret, C., Jaslin, G., and Scherman, D. (2000) Synthesis and biological properties of new glycosidic cationic lipids for DNA delivery. *Bioorg. Med. Chem. Lett. 10*, 1393–1395.

(25) Herscovici, J., Egron, M. J., Quenot, A., Leclercq, F., Leforestier, N., Mignet, N., Wetzer, B., and Scherman, D. (2001) Synthesis of new cationic lipids from unsaturated glycoside scaffold. *Org. Lett. 3* 1893–1896.

(26) Arigon, J., Prata, C. A. H., Grinstaff, M. W., and Barthélémy, P. (2005) Nucleic acid complexing glycosyl nucleoside-based amphiphile. *Bioconjugate Chem. 16*, 864–872.

(27) Prata, C. A. H., Zhang, X., Luo, D., McIntosh, T. J., Barthélémy, P., and Grinstaff, M. W. (2008) Lipophilic peptides for gene delivery. *Bioconjugate Chem. 19*, 418–420.

(28) Chan, E., Amon, M., Marano, R. J., Wimmer, N., Kearns, P. S., Manolios, N., Rakoczy, P. E., and Toth, I. (2007) Novel cationic lipophilic peptides for oligodeoxynucleotide delivery. *Bioorg. Med. Chem. 15*, 4091–4097.

(29) Montier, T., Benvegnu, T., Jaffres, P. A., Yaouanc, J. J., and Lehn, P. (2008) Progress in cationic lipid-mediated gene transfection: a series of bio-inspired lipids as an example. *Curr. Gene Ther. 8*, 296–312.

(30) Obata, Y., Suzuki, D., and Takeoka, S. (2008) Evaluation of cationic assemblies constructed with amino acid based lipids for plasmid DNA delivery. *Bioconjugate Chem. 19*, 1055–1063.

(31) Gissot, A., Camplo, M., Grinstaff, M. W., and Barthélémy, P. (2008) Nucleoside, nucleotide and oligonucleotide based amphiphiles: a successful marriage of nucleic acids with lipids. *Org. Biomol. Chem. 6*, 1324–1333.

(32) Moreau, L., Barthélémy, P., Maataoui, M. E., and Grinstaff, M. W. (2004) Supramolecular assemblies of nucleoside-based amphiphiles. *J. Am. Chem. Soc. 126*, 7533–7539.

(33) Moreau, L., Ziarelli, F., Grinstaff, M. W., and Barthélémy, P. (2006) Self-assembled microspheres from F-block elements and nucleoamphiphiles. *Chem. Commun. 15*, 1661–1663.

(34) Moreau, l., Campins, N., Grinstaff, M. W., and Barthélémy, P. (2006) A fluorocarbon nucleoamphiphile for the construction of actinide loaded microspheres. *Tetrahedron Lett. 47*, 7117–7120.

(35) Barthélémy, P., Prata, C. A. H., Filocamo, S. F., Immoos, C. E., Maynor, B. W., Hashmi, S. A. N., Lee, S. J., and Grinstaff, M. W. (2005) Supramolecular assemblies of DNA with neutral nucleoside amphiphiles. *Chem. Commun.* 1261–1263.

(36) Campins, N., Dieudonné, P., Grinstaff, M. W., and Barthélémy, P. (2007) Nanostructured assemblies from nucleotide based amphiphiles. *New. J. Chem. 31*, 1928–1934.

(37) Chabaud, P., Camplo, M., Payet, D., Serin, G., Moreau, L., Barthélémy, P., and Grinstaff, M. W. (2006) Cationic nucleoside lipids for gene delivery. *Bioconjugate Chem. 17*, 466–472.

(38) Moreau, L., Barthélémy, P., Li, Y., Luo, D., Prata, C. A. H., and Grinstaff, M. W. (2005) Nucleoside phosphocholine amphiphile for in vitro DNA transfection. *Mol. BioSystems 1*, 260–264.

(39) Camplo, M., Khiati, S., Ceballos, C., Prata, C. A. H., Giorgio, S., Marsal, P., Barthélémy, P., and Grinstaff, M. W. (2010) Cationic nucleoside lipids derived from universal bases: a rational approach for siRNA transfection. *Bioconjugate Chem. 21*, 1062–1069.

(40) Boomer, J. A., and Thompson, D. H. (1999) Synthesis of acid-labile diplasmenyl lipids for drug and gene delivery applications. *Chem. Phys. Lipids 99*, 145–153.

(41) Liu, X., Yang, J. W., and Lynn, D. M. (2008) Addition of 'charge-shifting' side chains to linear poly(ethyleneimine) enhances cell transfection efficiency. *Biomacromolecules 9*, 2063–2071.

(42) Bell, P. C., Bergsma, M., Dolbnya, I. P., Bras, W., Stuart, M. C., Rowan, A. E., Feiters, M. C., and Engberts, J. B. F. N. (2003) Transfection mediated by genimi Surfactants: Engineered escape from the endosomal compartment. *J. Am. Chem. Soc. 125*, 1551–1558.

(43) Lynn, D. M., and Langer, R. (2000) Degradable poly(beta-amino esters): Synthesis, characterization, and self-assembly with plasmid DNA. *J. Am. Chem. Soc. 122*, 10761–10768.

(44) Pack, D. W., Putnam, D., and Langer, R. (2000) Design of imidazole-containing endosomolytic biopolymers for gene delivery. *Biotechnol. Bioeng. 67*, 217–223.

(45) Jones, R. A., Cheung, C. Y., Black, F. E., Zia, J. K., Stayton, P. S., Hoffman, A. S., and Wilson, M. R. (2003) Poly(2-alkylacrylic acid) polymers deliver molecules to the cytosol by pH-sensitive disruption of endosomal vesicles. *Biochem. J. 372*, 65–75.

(46) Zhu, J., Munn, R. J., and Nantz, M. H. (2000) Self-cleaving ortho ester lipids: A new class of pH-vulnerable amphiphiles. *J. Am. Chem. Soc. 122*, 2645–2646.

(47) Jewell, C. M., Zhang, J., Fredin, N. J., Wolff, M. R., Hacker, T. A., and D.M., L. (2006) Release of plasmid DNA from intravascular stents coated with ultrathin multilayered polyelectrolyte films. *Biomacromolecules 7*, 2483–2491.

(48) Legendre, J. Y., and Szoka, F. C. J. (1992) Delivery of plasmid DNA into mammalian cell lines using pH sensitive liposomes: Comparison with cationic liposomes. *Pharm. Res. 10*, 1235–1242.

(49) Midoux, P., Pichon, C., Yaouanc, J. J., and Jaffrès, P. A. (2009) Chemical vectors for gene delivery: a current review on polymers, peptides and lipids containing histidine or imidazole as nucleic acids carriers. *Br. J. Pharmacol. 157*, 166–178.

(50) McGregor, C., Perrin, C., Monck, M., Camilleri, P., and Kirby, A. J. (2001) Rational apporaches to the design of cationic genimi surfactants for gene delivery. *J. Am. Chem. Soc. 123*, 6215–6220.

(51) Gosselin, M. A., Guo, W., and Lee, R. J. (2002) Incorporation of reversibly cross-linked polyplexes into LPDII vectors for gene delivery. *Bioconjugate Chem. 13*, 1044–1053.

(52) Tang, F., Wang, W., and Hughes, J. A. (1999) Cationic liposomes containing disuldide bonds in delivery of plasmid DNA. *J. Liposome Res. 9*, 331–347.

(53) Byk, G., Wetzer, B., Frederic, M., Dubertret, C., Pitard, B., Jaslin, G., and Scherman, D. (2000) Reduction-sensitive lipopolyamines as a novel nonviral gene delivery system for modulated release of DNA with improved transgene expression. *J. Med. Chem. 43*, 4377–4387.

(54) Prata, C. A. H., Zhao, Y., Barthélémy, B., Li, Y., Luo, D., McIntosh, T. J., Lee, S. J., and Grinstaff, M. W. (2004) Charge-reversal amphiphiles for gene delivery. *J. Am. Chem. Soc. 126*, 12744–12745.

(55) Abbott, N. L., Jewell, C. M., Hays, M. E., Kondo, Y., and Lynn, D. M. (2005) Ferrocene-containing cationic lipids: Influence of redox state on cell transfection. *J. Am. Chem. Soc. 127*, 11576–11577.

(56) Jewell, C. M., Hays, M. E., Kondo, Y., Abbott, N. L., and Lynn, D. M. (2008) Chemical activation of lipoplexes formed from DNA and a redox-active, ferrocene-containing cationic lipid. *Bioconjugate Chem. 19*, 2120–2128.

(57) Fuchs, S., Buethe, D., Khanna, A., Yadava, P., and Hughes, J. A. (2004) Sulfhydryl based cationic surfactants and the impact of polyanions on disulfide bond formation: Implications for gene transfer vectors. *J. Drug Targeting 12*, 347–353.

(58) Jewell, C. M., Hays, M. E., Kondo, Y., Abbott, N. L., and Lynn, D. M. (2006) Ferrocene-containing cationic lipids for the delivery of

DNA: Oxidation state determines transfection activity. *J. Controlled Release 112*, 129–138.

(59) Miyata, K., Kakizawa, Y., Nishiyama, N., Harada, A., Yamasaki, Y., Koyama, H., and Kataoka, K. (2004) Block catiomer polyplexes with regulated densities of charge and disulfide cross-linking directed to enhance gene expression. *J. Am. Chem. Soc. 126*, 2355–2361.

(60) Wang, J., Guo, X., Xu, Y., Barron, L., and Szoka, F. C. (1998) Synthesis and characterization of long chain alkyl acyl carnitine esters. Potentially biodegradable cationic lipids for use in gene delivery. *J. Med. Chem. 41*, 2207–2215.

(61) Pak, C. C., Ali, S., Janoff, A. S., and Meers, P. (1998) Triggerable liposomal fusion by enzyme cleavage of a novel peptide-lipid conjugate. *Biochem. Biophys. Acta 1372*, 13–27.

(62) Wang, J., Mao, H. Q., and Leong, K. W. (2001) A novel biodegradable gene carrier based on polyphosphoester. *J. Am. Chem. Soc. 123*, 9480–9481.

(63) Takeda, N., Nakamura, E., Yokoyama, M., and Teuro, O. (2004) Temperature-responsive polymeric carriers incorporating hydrophobic monomers for effective transfection in small doses. *J. Controlled Release 95*, 343–355.

(64) Kurisawa, M., Yokoyama, M., and Okano, T. (2000) Gene expression control by thermo-responsive polymeric gene carriers *J. Controlled Release 69*, 127–137.

(65) Prata, C. A. H., Li, Y., Luo, D., McIntosh, T. J., Barthélémy, P., and Grinstaff, M. W. (2008) A new helper phospholipids for gene delivery. *Chem. Commun.* 1566–1568.

(66) Zhang, X. X., Prata, C. A. H., McIntosh, T. J., Barthélémy, P., and Grinstaff, M. W. (2010) The effect of charge-reversal amphiphile spacer composition on DNA and siRNA delivery. *Bioconjugate Chem. 21*, 988–993.

(67) Mellman, I., Fuchs, R., and Helenius, A. (1986) Acidification of the endocytic and exocytic pathways. *Annu. Rev. Biochem. 55*, 663–700.

(68) Lavis, L. D., Chao, T. Y., and Raines, R. T. (2006) Fluorogenic label for biomolecular imaging. *ACS Chem. Biol. 1*, 252–260.

(69) Geall, A. J., and Blasgbrough, I. S. (2000) Rapid and sensitive ethidium bromide fluorescence quenching assay of polyamine conjugate-DNA interactions for the analysis of lipoplex formation in gene therapy. *J. Pharm. Biomed. Anal. 22*, 849–859.

(70) Cain, B. F., Baguley, B. C., and Demmy, M. W. (1978) Potential antitumor agents. 28. Deoxyribonucleic acid polyintercalating agents. *J. Med. Chem. 21*, 658–668.

(71) Koltover, I., Salditt, T., Radler, J. O., and Safinya, C. R. (1998) An inverted hexagonal phase of cationic liposome-DNA complexes related to DNA release and delivery. *Science 281*, 78–81.

(72) Liu, X. H., Yang, J. W., Miller, A. D., Nack, E. A., and Lynn, D. M. (2005) Charge-shifting cationic polymers that promote self-assembly and self-disassembly with DNA. *Macromolecules 38*, 7907–7914.